Pacific Northwest
NATIONAL LABORATORY

Online Monitoring of Medium Voltage Cable Systems with Spread Spectrum Time Domain and Frequency Domain Reflectometry

September 2023

S.W. Glass
J.R. Tedeschi
M.R. Huyge
M.P. Spencer
L.S. Fifield

DISCLAIMER

This report was prepared as an account of work sponsored by an agency of the United States Government. Neither the United States Government nor any agency thereof, nor Battelle Memorial Institute, nor any of their employees, makes **any warranty, express or implied, or assumes any legal liability or responsibility for the accuracy, completeness, or usefulness of any information, apparatus, product, or process disclosed, or represents that its use would not infringe privately owned rights**. Reference herein to any specific commercial product, process, or service by trade name, trademark, manufacturer, or otherwise does not necessarily constitute or imply its endorsement, recommendation, or favoring by the United States Government or any agency thereof, or Battelle Memorial Institute. The views and opinions of authors expressed herein do not necessarily state or reflect those of the United States Government or any agency thereof.

Online Monitoring of Medium Voltage Cable Systems with Spread Spectrum Time Domain and Frequency Domain Reflectometry

September 2023

S.W. Glass
J.R. Tedeschi
M.R. Huyge
M.P. Spencer
L.S. Fifield

Summary

In-service failures of wave energy convertor (WEC) cable systems can have a significant cost and power availability impact. Close parallel research of 2019 data showed > 1B£ and 9 Terra-Watt-Hours associated with global off-shore wind (OSW) cable failures (Strang-Moran 2020). It is likely these costs and availability will be amplified for wave energy converters if deployed in more energetic environments. OSW is a closely related technology but currently is significantly cheaper than WEC technology. For wave energy to compete, the problem of reliable cable transmission must be mitigated. This project develops isolation technology to allow online high frequency reflectometry testing of medium voltage cables (1 to 10 kV and higher) without arcing or damage to the test instrument.

Online spread spectrum time domain reflectometry (SSTDR) testing has been established for low voltage cable systems in the aircraft and rail industry and the ability to detect and locate cable flaws of interest is well understood. Extending reflectometry testing to medium voltage systems could enable detection of cable damage before failures occur thereby allowing repair and replacement of damaged cable segments to be scheduled and managed. The seedling project succeeded to pass and receive high frequency SSTDR signals onto a cable up to 1 kV using a parallel trace isolation circuit board that can be connected onto the test cable. The approach used a novel circuit design for which an invention disclosure has been filed. A proposed sapling project would extend the technology toward the higher operating voltages used by WEC systems, thereby enabling online SSTDR cable monitoring.

The goal of the seedling project was to extend the capability of the ARENA cable/motor test bed to address medium voltages and to develop a high pass filter isolation architecture to protect the reflectometry instrument from the low frequency (DC – 60 Hz) line voltage while allowing the high frequency diagnostic signal to pass to and from the test instrument to the live line. Initial efforts focused on passive LCR filter circuits to reduce 60 Hz levels below 10 volts from an 11.5 kV line while allowing the MHz high frequency chirps to pass onto the cables and for mV signals to be detected. We discovered that the parasitic loss behavior of real high voltage components precluded this approach from working.

An alternate approach was adapted for the electric field to couple between two parallel traces on a printed circuit board much like a radio-frequency coupler. The challenge here was and is to have the parallel traces close enough to each other to effectively pass the high frequency chirp onto the live line and receive any reflected signal from any encountered impedance change along the cable. This reflected signal will be in the mV range. The traces however must be far enough apart to not allow arcing on the board. A design with 3 mm spacing was determined to allow the high frequency signal to pass onto the live line and receive the mV signal back into the instrument while reducing the 60 Hz voltage amplitude by >80 dB (more than a factor of 10,000) without allowing arcing from across the parallel traces. This was confirmed by simulation and test.

Acknowledgments

Acronyms and Abbreviations

a.u.	arbitrary units: for this work a.u. is applied to dimensionless relative permittivity
AMP	aging management program
ARENA	Accelerated and Real-Time Environmental Nodal Assessment
AWG	Arbitrary Waveform Generator
BPSK	Binary Phase Shift Keying
dB	Decibels = $20 \log_{10}(V_{output}/V_{input})$
DFT	distance-to-fault
DOE	Department of Energy
EPRI	Electric Power Research Institute
Fc	Carrier Frequency
FDR	frequency domain reflectometry
FFT	fast Fourier transform
HFSS	ANSYS High Frequency Simulation Software
LWRS	Light Water Reactor Sustainability Program
MV	medium voltage
NDE	nondestructive evaluation
OSW	offshore wind
PNNL	Pacific Northwest National Laboratory
SSTDR	spread spectrum time domain reflectometry
TDR	time domain reflectometry
V	volt
VAC	volts alternating current
VNA	vector network analyzer
VOP	velocity of propagation

Contents

Figures

1.0 Introduction

Although detailed data on wave energy converter (WEC) cable system failures are limited, there are substantial data on off-shore wind system failures and specifically cable failures. In one UK study, off-shore wind energy generation cable failure losses for UK/Scotland were significant – more than 1 billion £s/yr. or more than 9 terawatt hours (Strang-Moran 2020). This project was focused on WEC systems rather than off-shore wind systems but the technology is similar and there are certainly parallels. Having a reliable online monitoring system that could warn of impending cable failures allowing load redistribution and managed repair can result in significant savings.
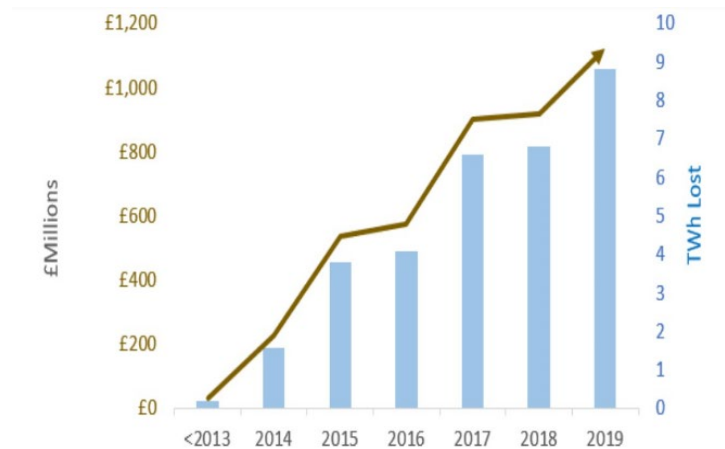

Figure 1. Cost of U.K. off-shore wind energy cable related failures from C. Strang-Moran, Offshore Renewable Energy Catapult, Glasgow, G1 1RD, Scotland https://wes.copernicus.org/preprints/wes-2020-56/wes-2020-56.pdf

Spread spectrum time domain reflectometry (SSTDR) is established for rail & aircraft but only for off-line and low voltage applications (Furse C. 2005). If the cable can be disconnected from the energized sources, tests can be applied to large diameter medium or high voltage systems. The SSTDR instruments are designed so that they can also be applied to low voltage systems below 1000 Volts (DC or 60 Hz). No commercial medium voltage live cable online monitoring solutions exist. For WEC cable systems, disconnection and re-connection for off-line testing is impractical and has seen limited industrial application. If an online medium voltage monitoring system were available to warn of cable damage prior to failure such that more focused inspection and repair can be scheduled and managed, significant cost savings can be realized.

This research effort was to develop an isolation circuit and test capability for spread spectrum time domain reflectometry (SSTDR) on medium voltage lines (2-35 kV).

2.0   Frequency Domain Reflectometry

Frequency domain reflectometry (FDR) is beginning to be used in nuclear plants particularly to locate areas of concern. The FDR instrument – typically a vector network analyzer or VNA is connected to two cable conductors – one considered the primary conductor under test and the other considered as the system ground as shown in (Figure 2) or to a parallel conductor within the cable bundle (Glass et al. 2017). The instrument directs a swept frequency chirp along the conductor and then listens for any reflection caused by an impedance change along the cable length. By listening and detecting the reflections in the frequency domain then transforming to the time domain with an IFT, significant noise immunity and sensitivity to subtle impedance changes can be achieved. Bandwidth for the FDR is software adjustable up to 1.3 GHz, but experience shows the best responses from 100 MHz to 500 MHz. Higher bandwidth FDR produces sharper peaks capable of spatially resolving more closely spaced impedance changes but the higher frequencies do not propagate as far along the cable length. FDR instruments are restricted to relatively low voltages and cannot tolerate testing on energized cable systems.
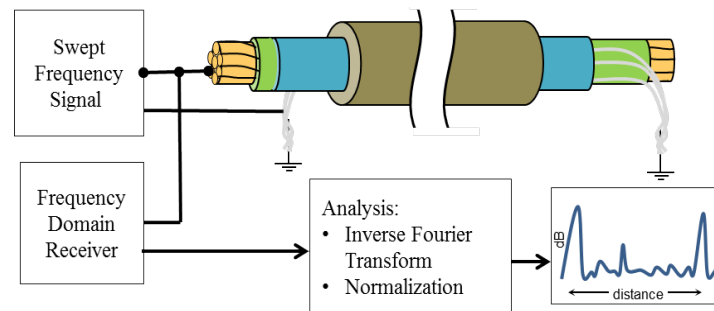

Figure 2. FDR cable testing introduces a swept frequency chirp onto a conductor then listens for any reflection from any impedance change along the cable length. Listening is captured in the frequency domain then transformed to time domain using an inverse Fourier transform (Glass et al. 2017).

3.0 Spread Spectrum Time Domain Reflectometry

The LIVEWIRE commercial SSTDR produces a similar plot to the laboratory VNA-based FDR however all processing is in the time domain. A pseudo-random noise code (PN code) is input onto the cable conductor and the instrument listens for any reflected response from cable anomalies. The SSTDR processes the signal as an autocorrelation comparing the input PN code to any reflected signal detected. The LIVEWIRE "Wilma" SSTDR model instrument used in these tests produced SSTDR spectra with bandwidths of 6,12,24, and 48 MHz. The autocorrelation algorithm produces a robust noise tolerant signal response, although indications from the 2022 study (Glass et al. 2022) showed the SSTDR data to be noisier than FDR data.
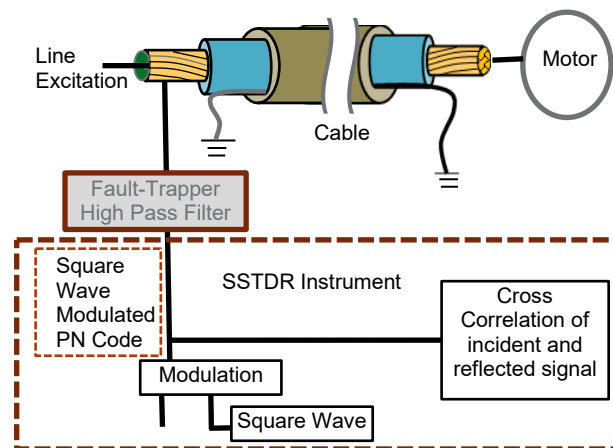

Figure 3. SSTDR Introduces a PN code high frequency signal modulated by a square Wave carrier onto the cable then listens for a reflection. Any reflection is cross correlated with the input for noise suppression.

4.0 Isolation Circuit Development Methodology and Simulated Performance

PNNL investigated multiple approaches to provide RF signals the ability to couple onto MV energized lines, while at the same time providing protection for the RF instrumentation from the MV 60 Hz signals. Three primary methods were evaluated: 1) discrete filter design, 2) magnetic field coupling, and 3) RF transmission line coupling.

Discrete filter design utilizes inductors and capacitors in a classical Chebyshev arrangement to create a 5th order high-pass filter circuit where the RF signals will couple onto the MV lines. Evaluation of the high-pass filter circuit was performed using Ansys simulation tools with first ideal inductors and capacitors, then with vendor provided data and simulated true component performance. In the ideal component case, the high pass filter circuit appeared to provide minimal loss (<6 dB) for the RF transmission and exceptional rejection for the 60 Hz MV signals (>100 dB), however as non-ideal characteristics were included in the model, such as the quality factor of the discrete components and the self-resonant frequencies, the filter performance became non-functional. This degraded performance for higher voltage rated components degraded signal quality for higher frequency operation. It is possible that state-of-the-art vendors such as Murata and Coilcraft will continue to develop product lines to support the MV applications, but no currently available component solutions were found that could solve this problem.

Investigation of magnetic field probe coupling was next evaluated. Magnetic field probes could provide the ability to selectively couple onto a selected line and it was demonstrated to have exceptional RF coupling, however it was determined that the topology of the magnetic field probe would require electrically shorting two of the MV conductors together which is not possible in practice.

The third and most promising coupling method thus far evaluated is electric field coupling using a microstrip directional coupler. Standard microstrip coupler designs are well published and utilized for coupling RF signals onto/off other RF signal lines. An adaptation of this architecture was developed that allowed MV signals to pass through one arm of the directional coupler and be electrically isolated from the RF. While the RF signals are injected/read out on a separate port and the transmission line runs parallel to the MV line for electric field coupling. Figure 4 below shows the coupling printed circuit board (PCB).
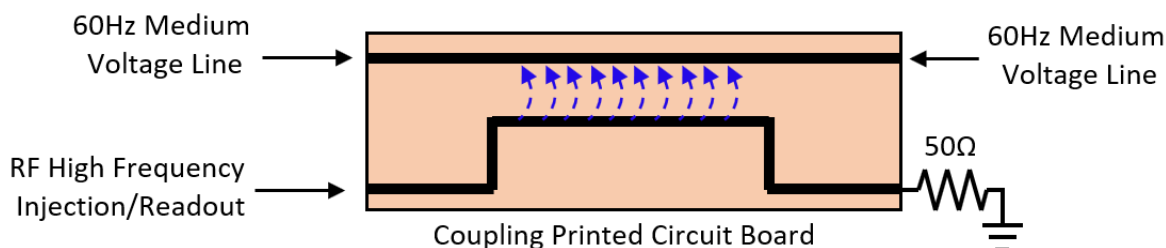

Figure 4. Coupling PCB showing electric field coupling between line trace and injection / readout trace

The design and simulation of the coupling PCB was first accomplished using ANSYS HFSS (Finite Element software) analysis as shown in (Figure 5). The simulated design incorporated the effects of the PCB material properties in the PCB as well as a conformal Kapton coating which improves the arc resistance of the PCB in accordance with (IPC 2012) for high-voltage circuit board conductor spacing/isolation requirements. The figure below shows the HFSS simulated PCB and the resulting coupled performance from the RF high frequency injection line to the 60 Hz medium voltage line.
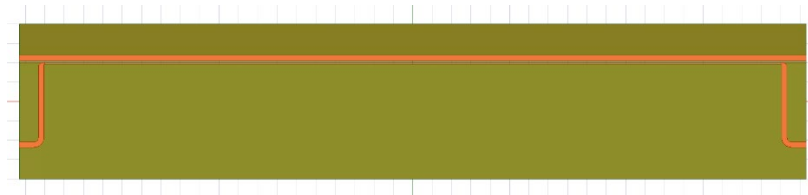

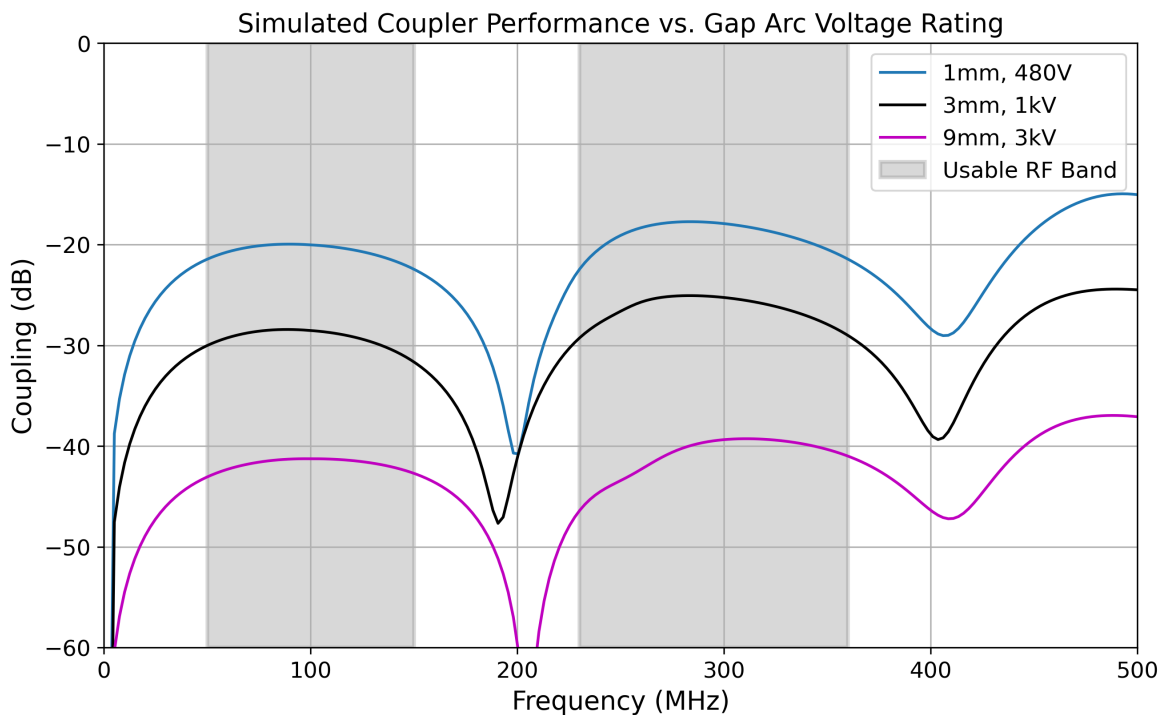Figure 5. HFSS Model of 1 mm Gap Coupling PCB

Figure 6. Simulated coupling performance from RF to 60 Hz Line with 1-, 3-, and 9-mm gap between line and instrument circuit board traces. The gaps determine the voltage rating that precludes arcing between traces.

The rejection of very low frequencies is shown for all permutations of the PCB, demonstrating that 60 Hz coupling between the MV and RF line on the PCB will be very low and protect the RF circuitry as intended. At higher frequencies, there are multiple bandwidths that are supported at approximately 100 MHz to 120 MHz wide, centered about 100 MHz and 300 MHz respectively. These usable bandwidths selected for SSTDR waveforms will be tuned and centered at the specific frequencies and take advantage of the good coupling in those frequency ranges. Figure 7 below shows an example of two SSTDR waveforms centered about the usable frequency ranges. Where a zoomed in plot of the time series is on the top, and the corresponding frequency spectrum for the full time series is below.
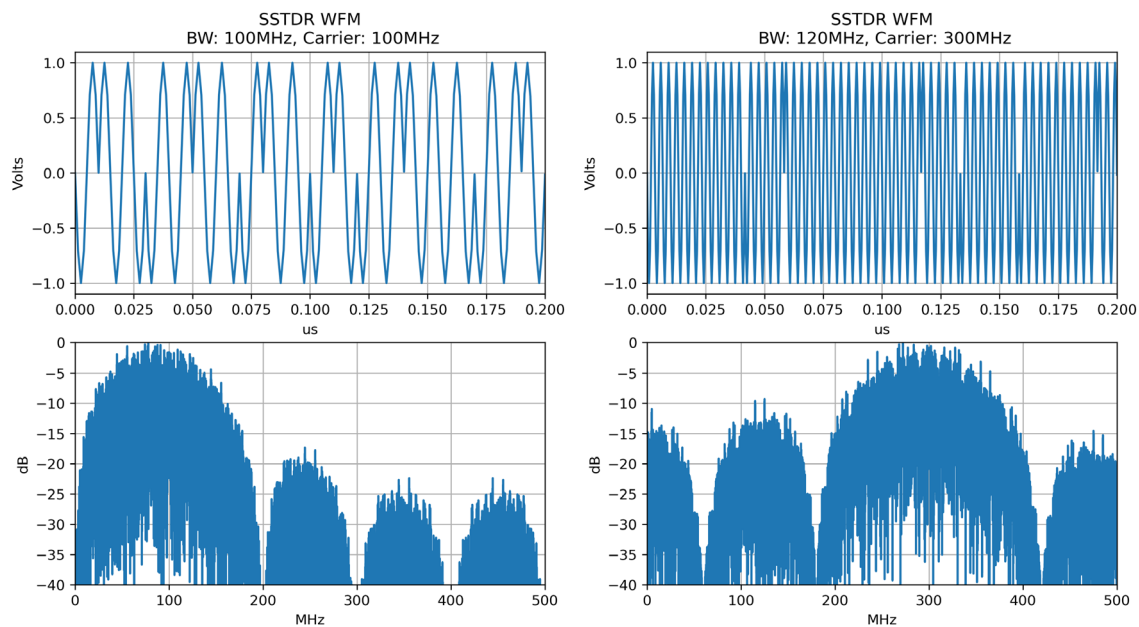
Figure 7. SSTDR waveforms centered about 100 MHz (left) and 300 MHz (right)

5.0 Test Results

5.1 FDR Response

Circuit boards with 1-mm, 3-mm, and 9-mm traces were fabricated and tested (Figure 8). Initial tests were performed to confirm the RF operation of the PCB. For testing the RF performance, a VNA was used measuring the FDR response of a 44-ft test cable with no live operating voltage. The FDR result, (Figure 9), clearly shows the start and end reflections of the 44-ft. test cable with a 10-ft lead. Because the temporal response corresponds to a specific distance along the cable, responses from motors, transformers, switches, or other components that produce a reflection are separated in time and corresponding distance along the cable from indications of interest. If flaws of interest however are near enough to cable ends or splices that produce large peaks, those large peaks can overshadow cable reflections from those flaws. Signal peak widths are generally a function of the reflectometry bandwidth. To aid signal interpretation, reflectometry measurements are taken at multiple bandwidths. Higher bandwidths have narrower peaks but are subject to greater noise and do not propagate as far down the cable due to attenuation. Lower bandwidth signals propagate farther with less noise, but response peaks from lower bandwidth signals are much broader. Reflectometry peaks measured with the isolation board in the circuit are somewhat broader than measurements without the isolation board and therefore signals from faults near the cable start and cable end or near other large reflectors may be obscured. The cable end reflections of Figure 9 are accentuated in the 44-ft. test cable because the end reflections cover a large portion of the FDR response, but these cable end indications would be less impactful as the cable lengths increase. Tests on longer cable lengths will have a noise floor similar to the baseline levels shown in Figure 9 for a majority of the cable and this test on shorter cable provides a generally encouraging result.

Figure 8.   Parallel trace circuit boards @ 1,3, and 9 mm corresponding to 0.5,1.0, and 3.0 kV arc threshold
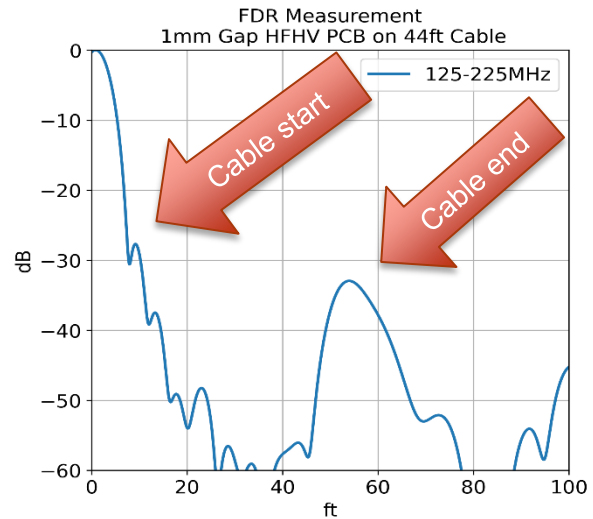

Figure 9.   FDR reflectometry signal on 50-ft. cable using the directional coupling parallel trace circuit board showing clear cable start and end responses with a manageable noise floor between the cable end responses

The bandwidth and center frequency of the reflectometry waveform was selected by a processing loop that cropped the complex frequency domain data to a selective bandwidth and carrier. The data was windowed, inverse Fourier transformed into the time domain, time shifted and normalized. This FDR data highlighting the ideal carrier and bandwidths of the fabricated coupler circuit will then be used to create optimized SSTDR waveforms in future evaluation.

5.2   60 Hz Voltage Attenuation

Additional testing was performed on the PCB to confirm the isolation of 60 Hz signals between the MV and RF lines. This was tested using a laboratory signal generator and oscilloscope as shown in Figure 10 to confirm the ratio of input to coupled 60 Hz signals. The input source into the MV 60 Hz line was a 10 V peak-to-peak waveform, and the output was measured at two ports, 1) through 60 Hz port and 2) the RF injection/reception port. The test results (Figure 11) show next to no loss for the 60 Hz signal traveling in the through port path, and for the 60 Hz into the RF port the measured voltage was less than 0.001 volts peak-to-peak (Vpp)(at the dynamic range limitations of the oscilloscope). This ratio of 10 Vpp to 0.001 Vpp equates to 20*log10(10/.001) = 80 dB or greater isolation between the two paths. This can then be extrapolated in a linear sense to higher voltages such as 10 kV peak-to-peak applied to the 60 Hz input would then produce a < 1 Vpp at the RF port which is suitable for RF test equipment. Note that additional 60 Hz coupling methods need to be considered such as dielectric breakdown and arcing with the higher voltages. These create additional means for the MV 60 Hz signals to leak onto the RF line and thus the reason for multiple PCB designs.
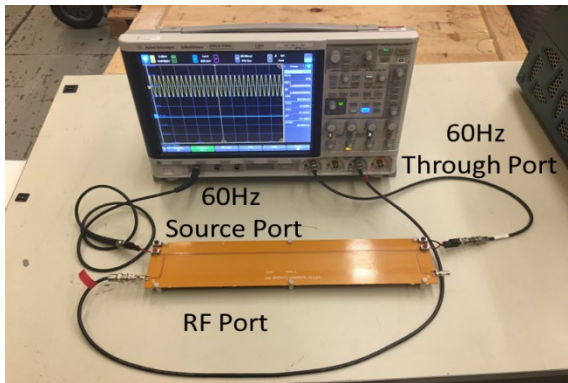
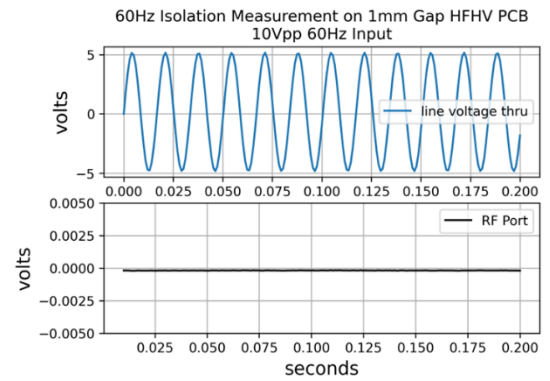Figure 10. Test setup for electrical isolation

Figure 11. Electrical isolation results – top shows 10-V P-P input; bottom shows < 0.001 V or -80-dB rejection

6.0   Observations and Conclusions

- Simple filter circuits applied at higher voltages (>1 kV) have parasitic losses that distort reflectometry wave forms and compromise SSTDR and FDR reflectometry tests.

- The parallel trace coupling technology is encouraging and offers a promising platform to build a medium voltage isolation circuit. Reflectometry signals were passed across the parallel trace coupling and cable end responses clearly detected cable ends indicating high likelihood of also detecting flaws of interest.

- The isolation circuit did broaden the reflectometry peaks compared to reflectometry indications without the isolation circuit. This will reduce flaw detection and resolution sensitivity. The degree of detection and resolution reduction when applied to a live wire test was not evaluated. Such an evaluation should be included in follow-on research.

- 60-Hz High voltage isolation of more than 80 dB was shown with the parallel trace circuit.

7.0   Plans Going Forward

For follow-on activities, we aim to extend to more WEC-relevant (higher) voltages utilized for linking WEC stations and transmitting WEC power by providing higher voltage isolation of the instrument while still effectively transmitting the high frequency reflectometry chirp to interrogate the cable for damage indications. Online real-time condition monitoring of live power cables for electrical fault detection using FDR and SSTDR can minimize operation, maintenance, and repair costs by detecting and locating cable damage before failure thereby allowing mitigation actions prior to a forced outage. Cable damage includes insulation thermal aging, moisture damage, mechanical fretting damage and low-resistance faults that manifest as an impedance change causing the reflectometry return signal. The parallel trace coupling circuit will be extended with voltage divider circuitry, active amplification, and other circuits applied to the lower voltage side of the system. The system will then be tested on medium voltage lines to demonstrate feasibility and pave the way for commercial implementation.

8.0 References

Furse C., Smith P., Safavi M. Lo C. 2005. "Feasibility of Spread Spectrum Sensors for Location of Arcs on Live Wires." *IEEE Sensors* 5 (6). 10.1109/JSEN.2005.858900

Glass, S W, A M Jones, L S Fifield, T S Hartman, and N Bowler. 2017. *Physics-Based Modeling of Cable Insulation Conditions for Frequency Domain Reflectometry (FDR).* PNNL-26493, Pacific Northwest National Laboratory, Richland, Washington. http://www.pnnl.gov/main/publications/external/technical_reports/PNNL-26493.pdf

IPC. 2012. "IPC 222-B 1Generic Standard for Printed Circuit Boards." Bannockburn, Illinois: Institute for Printed Circuit Boards. https://www.ipc.org/TOC/IPC-2221A.pdf

Strang-Moran, C. 2020. *Subsea Cable Management: Failure Trending for Offshore Wind.* *https://wes.copernicus.org/preprints/wes-2020-56/wes-2020-56.pdf*

Pacific Northwest
National Laboratory

902 Battelle Boulevard
P.O. Box 999
Richland, WA 99354

1-888-375-PNNL (7665)

www.pnnl.gov